Vol 16 No 12, December 2007
1009-1963/2007/16(12)/3747-07

Chinese Physics

© 2007 Chin. Phys. Soc.
and IOP Publishing Ltd

A simulation study of microstructure evolution during solidification process of liquid metal Ni*

Liu Hai-Rong(刘海蓉)[a], Liu Rang-Su(刘让苏)[b]†, Zhang Ai-Long(张爱龙)[a], Hou Zhao-Yang(侯兆阳)[b], Wang Xin(王 鑫)[b], and Tian Ze-An(田泽安)[b]

[a] *College of Materials Science and Chemical Engineering, Hunan University, Changsha* 410082, *China*
[b] *Department of Physics, Hunan University, Changsha* 410082, *China*

(Received 9 September 2007; revised manuscript received 21 September 2007)

A molecular dynamics simulation study has been performed for the microstructure evolution in a liquid metal Ni system during crystallization process at two cooling rates by adopting the embedded atom method (EAM) model potential. The bond-type index method of Honeycutt–Andersen (HA) and a new cluster-type index method (CTIM-2) have been used to detect and analyse the microstructures in this system. It is demonstrated that the cooling rate plays a critical role in the microstructure evolution: below the crystallization temperature T_c, the effects of cooling rate are very remarkable and can be fully displayed. At different cooling rates of $2.0 \times 10^{13}\,\mathrm{K \cdot s^{-1}}$ and $1.0 \times 10^{12}\,\mathrm{K \cdot s^{-1}}$, two different kinds of crystal structures are obtained in the system. The first one is the coexistence of the hcp (expressed by (12 0 0 0 6 6) in CTIM-2) and the fcc (12 0 0 0 12 0) basic clusters consisting of 1421 and 1422 bond-types, and the hcp basic cluster becomes the dominant one with decreasing temperature, the second one is mainly the fcc (12 0 0 0 12 0) basic clusters consisting of 1421 bond-type, and their crystallization temperatures T_c would be 1073 and 1173 K, respectively.

Keywords: liquid metal Ni, cooling rate, crystallization process, microstructure evolution, molecular dynamics simulation

PACC: 6120J, 6125M, 6470P, 7115Q

1. Introduction

The macro-properties of metal materials are mainly determined by their microstructures, and the microstructures are mainly related to the original configurations in liquid state and the solidification processes. For obtaining the microstructures with the best materials properties, it is necessary to make a tracing study on the microstructure transitions in solidification processes at different cooling rates. However, under the present experimental conditions, it is very difficult to perform a tracing study on the solidification process of liquid metal. With the development of computer technology, it is now possible to perform a tracing study by using molecular dynamics simulation and obtain a distinct physical picture for the solidification processes of liquid metal, and some important results have been obtained.[1−5]

At present, although some works have been devoted to the understanding of the solidification processes of liquid pure metal Ni,[6−8] the microscopic mechanism of structure evolution in solidification of liquid metal Ni is still not clear. Therefore, based on the previous works,[9−13] in this paper, by adopting the embedded atom method (EAM) potential, a molecular dynamics simulation for liquid metal Ni is performed at two different cooling rates and then the results are analysed by using the bond-type index method[14] and also the new cluster-type index method (CTIM-2). New information of microstructure evolution for liquid metal Ni is shown in the following Sections.

2. Simulation conditions and methods

Based on the density functional theory and the effective medium theory, Daw and Baskes[15] established a semi-empirical EAM model potential, which has been used successfully in the study of solid state matter at first and then extended to the research of liquid metals by Foiles.[16] As Foiles pointed out, there is a larger difference of the atomic distance between

*Project supported by the National Natural Science Foundation of China (Grant Nos 50271026 and 50571037).
†E-mail: liurangsu@sina.com

the liquid state and the solid state, therefore, the EAM potential formulation should be improved to meet the need of simulation of liquid metals as follows.

$$\rho_{h.i} = \bar{\rho} + \sum_{j<i} \left[\rho_j^a(R_{ij}) - \delta\right], \quad (1)$$

where $\rho_{h,i}$ is the electron density at the position of atom i, $\bar{\rho}$ is the average electron density in the liquid state, $\rho_j^{\mathrm{a}}(R_{ij})$ is the density of atom j around the position of atom i with a distance of r_{ij}, $\delta = \bar{\rho}/(N-1)$. The effective pair potential is given by

$$\psi(R) = \Phi(R) + 2F'(\bar{\rho})\rho_{\mathrm{a}}(R) + F''(\bar{\rho})[\rho_{\mathrm{a}}(R)]^2, \quad (2)$$

where $F(\rho)$ is the energy required to embed an atom i into the background electron density at site i, and $\Phi(r)$ is the pair potential. The EAM potential formulation is written as

$$E_{\mathrm{tot}} = \sum_i F_i(\rho_i) + \sum_{i<j} \Phi(r_{ij}), \quad (3)$$

$$F(\rho) = -F_0 \left[1 - \ln\left(\frac{\rho}{\rho_{\mathrm{e}}}\right)^n\right]\left(\frac{\rho}{\rho_{\mathrm{e}}}\right)^n + F_1\left(\frac{\rho}{\rho_{\mathrm{e}}}\right), \quad (4)$$

$$\Phi(r) = -\alpha\left[1 + \beta\left(\frac{r}{r_{\mathrm{a}}} - 1\right)\right] \times \exp\left[-\beta\left(\frac{r}{r_{\mathrm{a}}} - 1\right)\right], \quad (5)$$

$$\rho_i = \sum_{j\neq i} f(r_{ij}) = \sum_{j\neq i} f_{\mathrm{e}} \exp\left[-\chi(r - r_{\mathrm{e}})\right], \quad (6)$$

where E_{tot} is the total energy of a system, ρ_i is the linear superposition of the electron density surrounding each atom, α, β, F_0, F_1 are the fitting parameters same as in Ref.[17], $n = 0.5$.

The molecular dynamics (MD) technique and the simulation conditions used here are as follows: Firstly, 500 Ni atoms are randomly placed in a cubic box; and the system runs under periodic boundary conditions. The cubic box size is determined by both the number of atoms in the system and the mean volume of each atom at each given temperature.[18] The mean volume is changed with temperature; thus the box size will also be changed with temperature. The interaction potential adopted here is the effective EAM potential function mentioned above.

This simulation is started at 1973 K (the melt point of Ni is 1727 K). At this temperature, the system runs 100000 time steps to obtain equilibrium liquid state. Then the temperature of the system is decreased from 1973 to 373 K with a temperature internal of 100 K, using the damped force method,[4] at different cooling rates of 2×10^{13} and $1 \times 10^{12}\,\mathrm{K \cdot s^{-1}}$, respectively. After the system runs 3000 time steps we record the atom structural configurations of the system, i.e. the space coordinates of atoms at each given temperature. Finally, the microstructures in the system are detected by means of the bond-type index method of Honeycutt–Andersen (HA)[14] and the cluster-type index method (CTIM-2), and their evolution mechanisms are also discussed.

3. Simulation result analysis

3.1. Pair distribution function analysis

The pair distribution $g(r)$ is the Fourier transform of the structure factor $S(q)$ obtained by x-ray diffraction experiment. It has been an important method to compare the theoretical results with the experimental ones for liquid and amorphous structures at present. The comparison of $g(r)$ at 1873 K between the present simulated results and the experimental results of Waseda[19] is shown in Fig.1. From Fig.1, it can be clearly seen that they are in good agreement. Therefore, the effective EAM potential function adopted here is successful in reflecting the physical nature of this system, and we believe that the other simulation results is reliable as well.

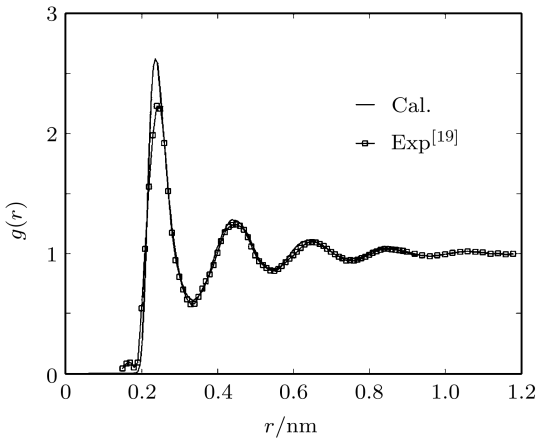


Fig.1. Comparison of the pair distribution function $g(r)$ of liquid Ni with the experimental result obtained at 1873 K.

3.2. Bond-type index analysis

In order to further understand the microstructures in the system, at present, the pair analysis technique, especially the bond-type index method of Honeycutt–Andersen (HA)[14] has been applied

widely, and become an important method for describing the microstructures of disordering systems, such as liquid, amorphous states and so on. According to the definition of the HA bond-type index, any pair of atoms under consideration in a system can be characterized by four numbers $ijkl$. The first number i is 1 if the root pair of atoms is bonded, or 2 otherwise. The second number j represents the number of near-neighbours shared by the root pair of interest. The third number k is the number of bonds between the shared neighbours. These three numbers are not sufficient to characterize a diagram uniquely, so a fourth number l is added to resolve the ambiguity about the arrangement of the atomic bonds. Applying this HA bond-type index, the bond-types between two atoms can be determined clearly. It is well known that described by bond-type index method of HA, each of the various systems has its own characteristic bond-type. For example, the 1551, 1541 and 1431 bond-types are characteristic bond-types of typical liquid and amorphous states; the 1661(six) and 1441(eight) bond-types are the characteristic bond-types of bcc crystal; the 1421(twelve) bond-type is the characteristic bond-type of fcc crystal, while for hcp crystal the characteristic bond-types are 1421(six) and 1422(six).

The relative number of seven main bond-types changed with temperature at different cooling rates of 2×10^{13} and $1 \times 10^{12}\,\mathrm{K \cdot s^{-1}}$ are shown in Figs.2(a) and 2(b) respectively. From these figures, it can be seen that when the temperature is above 1273 k, the effects of the two different cooling rates on the different bond-types are very small, and the variation trend is almost the same. But as the temperature decreases continually from 1173K, the effects of cooling rates on the relative number of various bond-types become remarkable, especially on the 1421 and 1422 bond-types whose number is the largest and plays a leading role in the transition of microstructures. Finally, the crystal structures are formed in the systems with 1421 and 1422 bond-types as the dominant types. The crystallization temperatures T_c are approximately equal to 1073–973 K and 1173–1073 K, respectively.

From all these results, similar to those we obtained for other cases,[10−13] it can be seen that the effects of different cooling rates on the microstructures of liquid and supercooled states are very small. However, the effects of them on solid (amorphous or crystal) states are very remarkable and can be fully displayed only nearby the liquid-solid transition points, namely, T_g for the amorphous formation processes or T_c for the crystallization processes.

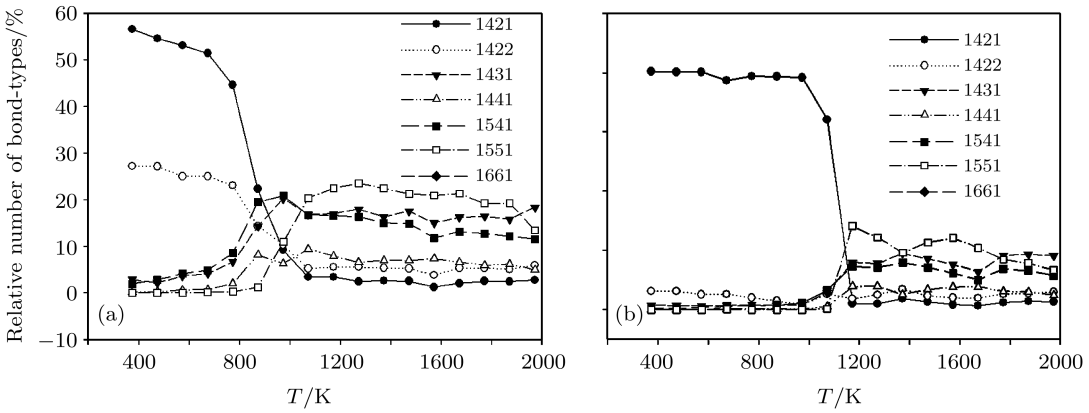


Fig.2. The relative number of bond-types changed with temperature at different cooling rate. (a) $2.0 \times 10^{13}\,\mathrm{K \cdot s^{-1}}$, (b) $1.0 \times 10^{12}\,\mathrm{K \cdot s^{-1}}$

3.3. Analyses of cluster structures

The structures of various clusters are formed by various special kinds and numbers of bond-types, however, at present, the bond-type index method of HA is very difficult to describe these clusters. In order to clearly describe all kinds of clusters, we have proposed a cluster-type index method (CTIM)[11−13] based on the HA indices[14] and the work of Qi and Wang.[20] We have defined the basic cluster as the smallest cluster composed of a core atom and its surrounding neighbouring atoms. A larger cluster can be formed by continuous expanding a basic cluster as the core, according to a certain rule, or by combining several basic clusters together.

According to the definition of a basic cluster, four

integers are also adopted to describe the basic clusters. The meaning of the four integers used in CTIM are as follows: the first integer represents the number of surrounding atoms which form a basic cluster with the central atom, i.e. the coordination number Z of the central atom; the second, third and fourth integers represent the numbers of 1441, 1551 and 1661 bond-types, respectively, by which the surrounding atoms are connected with the central atom of the basic cluster. For example, (12 0 12 0) stands for an icosahedral cluster that is composed of 13 atoms: the central atom is connected to the surrounding atoms through twelve 1551 bond-types (i.e., the coordination number of the central atom $Z = 12$); (13 1 10 2) stands for the defective polyhedron cluster composed of 14 atoms, the core atom is connected to the surrounding atoms with one 1441, ten 1551 and two 1661 bond-types (the coordination number $Z = 13$), and so on. The CTIM has been successfully used to describe various clusters in liquid and amorphous metals, from basic clusters to larger clusters, as those shown in Refs.[11, 12].

Using the CTIM, bcc crystal unit (basic cluster) can be expressed as (14 6 0 8) and many kinds of basic clusters in amorphous state can be represented in a simple way (for details see Refs.[11–13]). However, the familiar fcc basic cluster which is made up of twelve 1421 bond-types, and hcp basic cluster which is made up of six 1421 and six 1422 bond-types, still cannot be described. In order to clearly describe the fcc and hcp basic clusters, the CTIM should be extended by adding two integers (namely, the fifth and the sixth ones, which represent the numbers of 1421 and 1422 bond-types in a cluster, respectively). For convenience of discussion, the CTIM with 6 integers is called CTIM-2. In the CTIM-2, the basic cluster can be expressed as follows: the icosahedron (ico-cluster), bcc crystal unit (bcc-cluster), hcp crystal unit (hcp-cluster) and fcc crystal unit (fcc-cluster) can be expressed in turn by (12 0 12 0 0 0), (14 6 0 8 0 0), (12 0 0 0 6 6) and (12 0 0 0 12 0), respectively. Their typical configurations are shown in Fig.3.

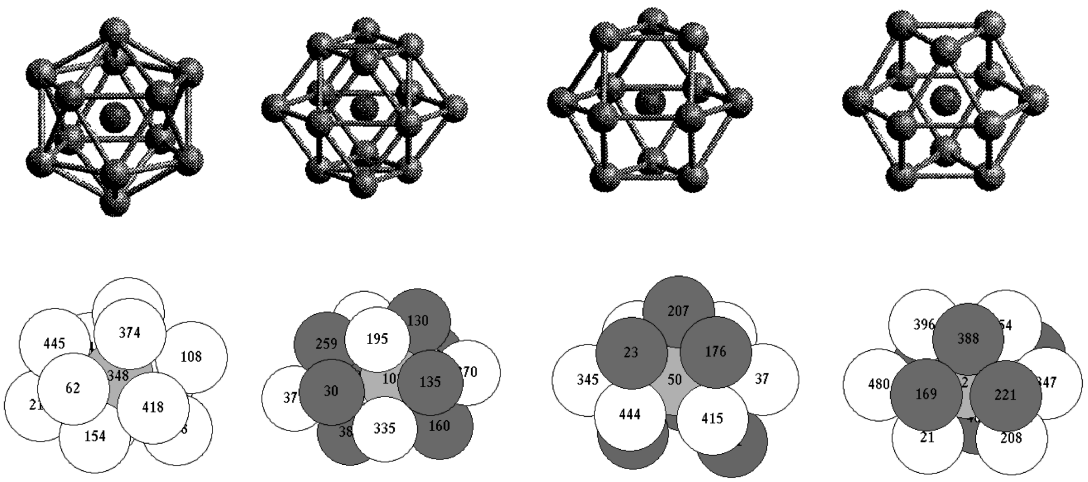


Fig.3. Schematic diagrams of the typical ico, dec, bcc, hcp and fcc basic clusters and the corresponding basic clusters found in the system expressed by CTIM-2.

For understanding the atomic distribution in the system, the whole schematic diagrams of the (100) cross section of the system at 373 K for cooling rate of 2.0×10^{13} and $1.0 \times 10^{12}\,\mathrm{K \cdot s^{-1}}$ are shown in Figs.4(a) and 4(b), respectively. It can be seen that the regular arrangements of crystal structures indeed have been formed in the two systems, especially, a typical fcc (12 0 0 0 12 0) structure has been formed in Fig.4(b).

For revealing the crystallization process of liquid Ni, the details of the evolution processes of various clusters in solidification at different cooling rates of 2.0×10^{13} and $1.0 \times 10^{12}\,\mathrm{K \cdot s^{-1}}$, are listed in Tables 1 and 2, respectively, from which, it can be clearly seen that during the two solidification processes, the crystallization temperature T_c are approximately 1073–973K and 1173–1073K, respectively. These results are in good agreement with those obtained from the HA bond-type indices analysis. In particular, from Table 1, it can be clearly seen the three basic clusters of icosahedron (12 0 12 0 0 0), hcp (12 0 0 0 6 6) and fcc (12 0 0 0 12 0) can coexist in the system at $T_c \approx 973$ K, while at 873 K and below only the hcp and fcc basic

clusters coexist and the hcp basic cluster becomes the dominant one with decreasing temperature. However, Table 2 shows that there is no coexistence of the three basic clusters of ico, hcp and fcc in the solidification process at $T_c \approx 1073\,\mathrm{K}$, only the hcp and fcc basic clusters coexist, and the dominant cluster has turned to be the fcc basic cluster at 1073 K and thereafter.

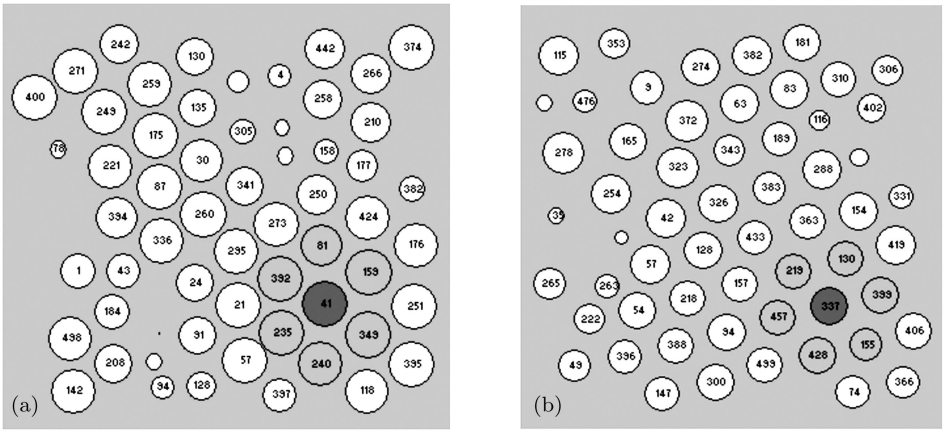


Fig.4. Fig. 4 Schematic diagrams of atomic distribution in cross section (100) in the system at 373 K for cooling rates: (a) $2.0 \times 10^{13}\,\mathrm{K \cdot s^{-1}}$; (b) $1.0 \times 10^{12}\,\mathrm{K \cdot s^{-1}}$.

Table 1. Variation of the number of clusters with temperature (K) at a cooling rate of $2.0 \times 10^{13}\,\mathrm{K \cdot s^{-1}}$.

Types of clusters	Temperature (K) and the number of various cluster-types													
	1973	1773	1573	1373	1273	1173	1073	973	873	773	673	573	473	373
(12 0 0 0 6 6)	0	0	0	0	0	0	0	0.5	28.5	121	148	158	181	187
(12 0 0 0 12 0)	0	0	0	0	0	0	0	0.5	15.5	81.5	104	113	122	132
(12 0 12 0 0 0)	0	1.5	1.5	3.0	4.0	1.0	0.5	0.5	0	0	0	0	0	0
(14 0 12 2 0 0)	0	0.5	0	0	0	1.0	0	0	0	0	0	0	0	0
(15 0 12 3 0 0)	0	0	0	0	0	0	0.5	0	0	0	0	0	0	0
(13 1 10 2 0 0)	0.5	2.5	3.0	5.0	4.5	5.0	4.0	0.5	0	0	0	0	0	0
(14 1 10 3 0 0)	0	0	2.5	0	2.5	0.5	0.5	0	0	0	0	0	0	0
(15 1 10 4 0 0)	0	1.0	0	1.0	0	0	0.5	0	0	0	0	0	0	0
(11 2 8 1 0 0)	0	0.5	0.5	0	0	0	0	0	0	0	0	0	0	0
(12 2 8 2 0 0)	.0.5	1.0	1.5	1.0	3.0	2.0	1.5	0	0	0	0	0	0	0
(13 2 8 3 0 0)	0.5	0	0.5	0	0	0.5	0.5	0.5	0	0	0	0	0	0
(14 2 8 4 0 0)	1.0	1.0	1.5	3.5	4.0	2.5	2.5	0.5	0	0	0	0	0	0
(15 2 8 5 0 0)	0	0	0.5	1.5	0.5	1.0	1.5	0	0	0	0	0	0	0
(16 2 8 6 0 0)	0	0.5	0	0	0	0	0	0	0	0	0	0	0	0
(12 3 6 3 0 0)	0.5	1.0	1.5	0	0	0.5	0	0	0	0	0	0	0	0
(13 3 6 4 0 0)	0	2.0	0.5	1.5	3.0	4.0	6.0	0	0	0	0	0	0	0
(14 3 6 5 0 0)	0.5	1.0	0.5	1.5	1.0	2.0	3.5	0	0	0	0	0	0	0
(15 3 6 6 0 0)	0	0.5	0.5	0.5	0	0.5	0	0	0	0	0	0	0	0
(12 4 4 4 0 0)	0	0	0	0.5	1.0	0	0	0	0	0	0	0	0	0
(13 4 4 5 0 0)	0	1.0	0	0	0	0.5	0.5	0	0	0	0	0	0	0
(14 4 4 6 0 0)	0	0	0	3.5	3.0	3.5	5.0	0.5	0.5	0	0	0	0	0
(15 4 4 7 0 0)	0	0	0	1.0	0	0	0.5	0	0	0	0	0	0	0
(12 5 2 5 0 0)	0	0	0	1.0	0	1.0	0	0	0	0	0	0	0	0
(13 5 2 6 0 0)	0	0	0	0.5	0	0.5	0.5	0	1.5	0	0	0	0	0
(15 5 2 8 0 0)	0	0	0	0	0	0	0	0	0.5	0	0	0	0	0
(14 6 0 8 0 0)	0	0	0	0	0	3.5	3.5	1.0	2.0	0	0	0	0	0
Total number of all clusters	3.5	12.0	14.5	25.0	26.5	29.5	31.5	4.5	48.5	202	252	271	303	319

Table 2. Variation of the number of clusters with temperatures (K) at a cooling rate of $1.0 \times 10^{12}\ \mathrm{K \cdot s^{-1}}$.

Types of clusters	Temperature (K) and the number of various cluster-types													
	1973	1773	1573	1373	1273	1173	1073	973	873	773	673	573	473	373
(12 0 0 0 6 6)	0	0	0	0	0	0	6.5	0	1.5	2	9.5	7	16	15
(12 0 0 0 12 0)	0	0	0	0	0	0	190	280.	302.	312.	304.	328.	327	330
(12 0 12 0 0 0)	0	2.5	2.0	2.0	2.0	2.0	0	0	0	0	0	0	0	0
(14 0 12 2 0 0)	0	0	1.5	0	0	0	0	0	0	0	0	0	0	0
(13 1 10 2 0 0)	0.5	1.5	3.5	2.0	3.0	6.0	0	0	0	0	0	0	0	0
(14 1 10 3 0 0)	0	0	1.5	2.5	0	0	0	0	0	0	0	0	0	0
(15 1 10 4 0 0)	0	0	0	1.5	0	6.0	0	0	0	0	0	0	0	0
(16 1 10 5 0 0)	0	0	1.5	1.0	0	0.5	0	0	0	0	0	0	0	0
(17 1 10 6 0 0)	0	0	0.5	0	0	0	0	0	0	0	0	0	0	0
(11 2 8 1 0 0)	0	0	0	1.0	0	0	0	0	0	0	0	0	0	0
(12 2 8 2 0 0)	0.5	1.5	0.5	1.0	1.0	4.5	0	0	0	0	0	0	0	0
(13 2 8 3 0 0)	0.5	0	2.5	0	2.5	0	0	0	0	0	0	0	0	0
(14 2 8 4 0 0)	1.0	1.0	1.5	1.5	3.5	6.5	0	0	0	0	0	0	0	0
(15 2 8 5 0 0)	0	0.5	0	0	2.0	1.5	0	0	0	0	0	0	0	0
(16 2 8 6 0 0)	0	0	0	0	0	0.5	0	0	0	0	0	0	0	0
(12 3 6 3 0 0)	0.5	0	0	0	0	0.5	0	0	0	0	0	0	0	0
(13 3 6 4 0 0)	0	0	4.0	0	6.0	3.5	0	0	0	0	0	0	0	0
(14 3 6 5 0 0)	0.5	0	1.0	1.0	4.5	3.0	0	0	0	0	0	0	0	0
(15 3 6 6 0 0)	0	0	0	0	0	0.5	0	0	0	0	0	0	0	0
(16 3 6 7 0 0)	0	0	0	0	0	0	0	0	0	0	0	0	0	0
(12 4 4 4 0 0)	0	0	1.0	0	0	0	0	0	0	0	0	0	0	0
(13 4 4 5 0 0)	0	0.5	0.5	0	0	1.0	0	0	0	0	0	0	0	0
(14 4 4 6 0 0)	0	0.5	1.5	1.0	2.0	5.5	0	0	0	0	0	0	0	0
(15 4 4 7 0 0)	0	1.0	2.0	1.0	0.5	4.5	0	0	0	0	0	0	0	0
(13 5 2 6 0 0)	0	0	0	0	0	0.5	0	0	0	0	0	0	0	0
Total number of all clusters	3.5	9.0	25.0	15.5	27.0	46.0	196.	280	303.	314	313	335	343	345

From these results, it is also obvious that above the liquid-solid transition temperature T_c, in liquid and supercooled states, the effects of different cooling rates on the numbers of basic clusters of liquid metal are very small, however, below the liquid-solid transition temperature, their effects are very remarkable and can be fully displayed. Thus the cluster-type index method (CTIM-2) used here is successful and would be a new approach to study the microstructure transition of liquid metals during solidification processes.

As for why the effects of different cooling rates on the microstructures can be fully displayed only at temperatures nearby the liquid-solid transition, we think that the main cause is as follows: during the solidification process of liquid metals studied as a function of time and the dimension of the clusters, when the temperature is above the liquid-solid transition temperature, the energy of atoms in the system is higher, and it is easier for the atoms to flow and diffuse. Thus atomic bonds may break and form new ones due to thermal fluctuations, and the microstructures in the system will be transferred frequently, so that the short-range-order structures, clusters, would be continuously formed, then decomposed, and re-formed as different clusters to adapt to the change of temperature. But this process is transitory, and the transition of short-range-order structures or clusters, is instantaneous, so the system is always in the approach to an equilibrium relevant to that temperature. Thus when the temperature is above the liquid-solid transition temperature, namely in liquid or superheated states, the effects of cooling rate on the microstructures are very small. However, when the temperature decreases continually from the liquid-solid transition temperature, the atoms cannot flow freely, and the diffuse mechanism also would be changed. The transfer of atoms becomes very slow, and the time needed for the processes of forming, decomposing and re-forming of clusters becomes longer and longer. It is unlikely

that the transitions in liquid and supercooled states can be rapidly adapted to the change of temperature, so the effects of cooling rate on the transitions of microstructures become more and more remarkable, and can be fully displayed. The mechanism of these effects will be discussed in another paper.

4. Conclusions

From the results and discussions, for the microstructure evolution during the solidification processes of liquid metal Ni, the conclusions can be drawn as follows:

1. During the solidification processes of liquid metal, for the cooling rates $2.0 \times 10^{13}\,\mathrm{K \cdot s^{-1}}$ and $1.0 \times 10^{12}\,\mathrm{K \cdot s^{-1}}$, two different kinds of crystal structures are formed in the system. The first one obtained at the former cooling rate is the coexistence of the hcp (expressed by (12 0 0 0 6 6) in CTIM-2) and the fcc (12 0 0 0 12 0) basic clusters consisting of 1421 and 1422 bond-types. The hcp basic cluster becomes the dominant one with decreasing temperature; the second one is mainly the fcc (12 0 0 0 12 0) basic clusters consisting of 1421 bond-type

2. Above the liquid-solid transition temperature T_c, in liquid and supercooled states, the effects of different cooling rates on the microstructures of liquid metal are very small; below the liquid-solid transition temperature, the effects of those are very remarkable and can be fully displayed. According to these features, it is possible to establish a new method for determining the crystallization temperature T_c of liquid metals.

3. The cluster-type index method (GTIM-2) is better than bond-type index method for further investigating the concrete structural characteristics of the disordering liquid, amorphous and some crystallization systems. This method would benefit the study on the transition mechanisms of the microstructures during the crystallization process of liquid metal.

References

[1] Qi Y, Cagin T, Yoshitaka K and William A G 1999 *Phys. Rev.* B **59** 3527

[2] Li H, Wang, G H, Ding F, Wang J L and Shen W F 2001 *Phys. Lett.* A **280** 325

[3] Chen J, Chen D Q and Zhang J L 2007 *Chin. Phys.* **16** 2779

[4] Liu R S, Qi D W and Wang S 1992 *Phys. Rev.* B **45** 451

[5] Zhao J Z, Liu J, Zhao Y and Hu Z Q 2007 *Acta Phys. Sin.* **56** 443 (in Chinese)

[6] van Swygenhoven H, Spaczer M and Caro A 1999 *Nanostructured Materials* **12** 629

[7] Alemany M M G, Rey C and Gallego L J 1998 *Phys. Rev.* B **58** 685

[8] Cherne F J and Baskes M I 2001 *Phys. Rev.* B **65** 024209

[9] Liu R S and Wang S 1992 *Phys. Rev.* B **46** 12001

[10] Liu R S, Li J Y, Dong K J, Zheng C X and Liu H R 2002 *Mater. Sci. Eng.* B **94** 141

[11] Dong K J, Liu R S, Yu A B, Zou R P and Li J Y 2003 *J. Phys.: Condens. Matter* **15** 743

[12] Liu R S, Dong K J, Li J Y, Yu A B and Zou R P 2005 *J. Non-Cryst. Solids* **351** 612

[13] Liu R S, Dong K J, Tian Z A, Liu H R and Peng P 2007 *J. Phys.:Condens. Matter* **19** 196103

[14] Honeycutt J D and Andersen H C 1987 *J. Phys. Chem.* **91** 4950

[15] Daw M S and Baskes M I 1984 *Phys. Rev.* B **29** 6443

[16] Foiles S M 1985 *Phys. Rev.* B **32** 3409

[17] Cai J and Ye Y Y 1996 *Phys. Rev.* B **54** 8398

[18] Qi D W and Wang S 1991 *J. Non-Cryst. Solids* **135** 73

[19] Waseda Y 1980 *The Structure of Non-crystalline Materials* (New York: McGraw-Hill) 270

[20] Qi D W and Wang S 1991 *Phys Rev.* B **44** 884